Small-Angle Neutron-Scattering and Viscosity Studies of CTAB/NaSal Viscoelastic Micellar Solutions

V. K. Aswal* and P. S. Goyal

Solid State Physics Division, Bhabha Atomic Research Centre, Mumbai 400 085, India

P. Thiyagarajan

Intense Pulsed Neutron Source, Argonne National Laboratory, Argonne, Illinois 60439

Received: November 12, 1997; In Final Form: January 7, 1998

Micellar solutions of cationic surfactant cetyltrimethylammonium bromide (CTAB) in the presence of sodium salicylate (NaSal) show a viscoelastic behavior. Small-angle neutron-scattering (SANS) and viscosity studies from CTAB/NaSal micellar solutions are reported. Zero-shear viscosity of these solutions as a function of NaSal concentration (C_s), at all the four measured surfactant concentrations (C_d) of 12.5. 25, 50 and 100 mM, show a double-peak behavior. The effect of C_s/C_d on two viscosity maxima and a minimum has been examined, and the scaling relations are obtained. SANS experiments have been carried out at different NaSal concentrations, beyond the first viscosity maximum for two surfactant concentrations of 25 and 100 mM. It is found that micelles are rigid rods and their exponential length distribution shows that they behave as living polymers beyond the first viscosity maximum. The micellar structure does not change in the living polymer regime, whereas viscosity varies with increase in NaSal concentration. The variation in viscosity seems to be connected with the change in the intermicelle interactions.

Introduction

Surfactant molecules self-assemble into aggregates in aqueous solution to form micelles above the critical micelle concentration. In general, the aggregates are globular micelles. It is known that micelles of cationic surfactants (e.g., cetyltrimethylammonium bromide (CTAB)) grow from globular to wormlike shapes on the addition of salts, such as KBr, NaSal (sodium salicylate), etc. Halide anions associate only moderately with surfactant cations, and the micellar growth is gradual. However, with anions that associate strongly with surfactant cations, such as salicylate (Sal^-), wormlike micelles grow rapidly even at low surfactant and salt concentrations. These solutions exhibit striking viscoelastic behavior.[1−8]

The zero-shear viscosity (η) of CTAB/NaSal solutions as a function of NaSal concentration (C_s) show two pronounced maxima.[9] At low NaSal concentrations, the solutions contain slightly elongated micelles and their contribution to the viscosity is small.[10] As the NaSal concentration is increased, the micelles grow in length and begin to overlap and entangle one another, leading to a large increase in viscosity.[11,12] It is believed that micelles have attained their full length at the first viscosity maximum and the system is entangled with a three-dimensional network. The reasons for the double-peak behavior of the η vs C_s curves in these solutions are not completely understood. However, there are certain conjectures that beyond the first viscosity maximum micelles behave like living polymers and the second peak in the viscosity is perhaps connected with the charge reversal owing to counterion condensation on the micelles. In the living polymer regime, micelles break and coalesce on a time scale smaller than the time scale of diffusional motion.[1,13] Theoretical models predict that micelles are highly polydispersed in this regime and their length distribution is exponential.[1] It is of interest to understand the viscosity of these solutions in terms of micellar structure and intermicellar interactions.

The structures of micelles in a number of aqueous solutions showing viscoelastic behavior have been investigated by cryo-transmission electron microscopy (cryo-TEM),[11,14−16] and by small-angle neutron scattering (SANS).[17−20] The most studied micellar solutions are CTAB, cetyltrimethylammonium chloride (CTAC), or cetylpyridinium bromide (CPyB) with NaSal, etc. Cryo-TEM measurements from these solutions clearly show the transition of globular micelles to wormlike or threadlike micelles with the increase in the NaSal concentration. This explains the rise in the viscosity because of the entanglement of the wormlike micelles up to the first viscosity maximum. Thereafter, however, rheological properties change as a function of NaSal concentration, whereas the electron micrographs all show similar images of entangled wormlike micelles.[14] The reasons for the same are not explained by these measurements.

So far, most of the SANS studies from viscoelastic micellar solutions have been reported on low salt concentrations. The existence of rodlike micelles in viscoelastic solutions have also been established by SANS studies.[17,18] Lin et al.[20] carried out both SANS and light-scattering studies from dilute viscoelastic solutions and concluded that micelles are rigid rods in these solutions. SANS studies were, however, confined to dilute solutions, and no attempt has been made to correlate the structure and the viscosity of the viscoelastic solutions. Preliminary SANS results on CTAB/NaSal solutions showed the wormlike micelles behave as a living polymers beyond the first viscosity maximum.[9] The measurements were made at high surfactant concentration and for a limited number of NaSal concentrations.

* To whom correspondence should be addressed. Fax: 91-22-5560750. E-mail: sspd@magnum.barc.ernet.in.

S1089-5647(98)00181-3 CCC: $15.00
Published on Web 03/17/1998

Because of the presence of the interparticle interference effect at high surfactant concentration, the analysis of SANS data, however, becomes difficult, and one is not sure if the derived parameters are dependable.

This paper reports the SANS and viscosity studies performed at different surfactant concentrations from CTAB/NaSal solutions as a function of NaSal concentration. The effect of surfactant concentration on the double-peak behavior in η vs C_s curves has been examined. SANS measurements were carried out for several NaSal concentrations to understand the viscosity behavior in the viscoelastic solutions, beyond the first viscosity maximum in η vs C_s curves. These measurements include measurements at low surfactant concentration, where the interparticle interference effect can be neglected.

Experiment

CTAB (99%) was bought from Sigma and NaSal (>99.5%) from Fluka and used as supplied. Micellar solutions were prepared in D_2O. In neutron experiments use of D_2O, instead of H_2O, provides better contrast between the micelles and the solvent. The zero-shear viscosity of CTAB/NaSal solutions were measured using Brookfield cone/plate viscometer. The measurements were made at four surfactant concentrations of 12.5, 25, 50, and 100 mM as a function of NaSal concentration. SANS experiments were performed at the Intense Pulsed Neutron Source at Argonne National Laboratory, Argonne, IL, using the small-angle diffractometer.[21] SANS measurements were made for two surfactant concentrations of 25 and 100 mM with different NaSal concentrations selected from viscosity curves. The solutions were held in a quartz sample holder, the thickness being 2 mm. The data were recorded in the Q-range of 0.006−0.24 Å^{-1}. The temperature was maintained at 35 °C, in both SANS and viscosity experiments. The measured SANS distributions have been corrected and normalized to a cross-sectional unit, using standard procedures.

SANS Analysis

The coherent differential scattering cross section ($d\Sigma/d\Omega$) for a solution of monodispersed interacting micelles can be expressed as[22]

$$\frac{d\Sigma}{d\Omega} = n(\rho_m - \rho_s)^2 V^2[\langle F^2(Q)\rangle + \langle F(Q)\rangle^2(S(Q) - 1)] + B \quad (1)$$

The same expression for noninteracting micelles (i.e., $S(Q) \sim 1$) is given by

$$\frac{d\Sigma}{d\Omega} = n(\rho_m - \rho_s)^2 V^2 \langle F^2(Q)\rangle + B \quad (2)$$

where n denotes the number density of the micelles, ρ_m and ρ_s are, respectively, the scattering-length densities of the micelle and the solvent, and V is the volume of the micelle. $F(Q)$ is the single particle form factor, and $S(Q)$ is the interparticle structure factor. B is a constant term that represents the incoherent scattering background, which is mainly due to hydrogen in the sample.

The intraparticle structure factor for a rodlike micelle of length $L = 2l$ and radius R is given by[23]

$$\langle F^2(Q)\rangle = \int_0^{\pi/2} \frac{\sin^2(Ql\cos\beta)}{q^2 l^2 \cos^2\beta} \frac{4J_1^2(QR\sin\beta)}{q^2R^2\sin^2\beta} \sin\beta\, d\beta \quad (3)$$

where β is the angle between the axis of the cylinder and the bisectrix. J_1 is the Bessel function of order unity. In case of long rodlike micelles ($L \gg R$), eq 3 reduces to the form

$$\langle F^2(Q)\rangle = \frac{\pi}{2QL} \exp\left(\frac{-Q^2R^2}{4}\right) \quad (4)$$

This equation shows that $\langle F^2(Q)\rangle$ will vary as $1/Q$ in the Q-range of $1/l < Q < 1/R$ for long rodlike micelles.

The radius of the rodlike micelles has a value that is nearly equal to the length of the surfactant molecule. The polydispersity in these solutions is expected to be only in the length of the micelles. In that case eq 2 for polydispersed solution can be written as

$$\frac{d\Sigma}{d\Omega} = (\rho_m - \rho_s)^2 \int n(L)\, V^2(L) \langle F^2(Q)\rangle f(L)\, dL + B \quad (5)$$

where $f(L)$ gives the length distribution of the micelles. Usually the Schultz distribution is assumed for the polydispersity.[24] The Schultz distribution is given by

$$f(L) = \left(\frac{Z+1}{\bar{L}}\right)^{Z+1} L^Z \exp\left[-\left(\frac{Z+1}{\bar{L}}\right)L\right] \frac{1}{\Gamma(Z+1)} \quad (6)$$

where $\bar{L}$ is the mean of the distribution and Z is the width parameter. The relative spread in the length of the distribution is given by

$$\frac{\Delta L}{\bar{L}} = \frac{1}{(Z+1)^{1/2}} \quad (7)$$

For the highly polydispersed solutions, $\Delta L/\bar{L} = 1$, when $Z = 0$. The Schultz distribution reduces to the exponential distribution as given by

$$f(L) = \frac{1}{\bar{L}} \exp(-L/\bar{L}) \quad (8)$$

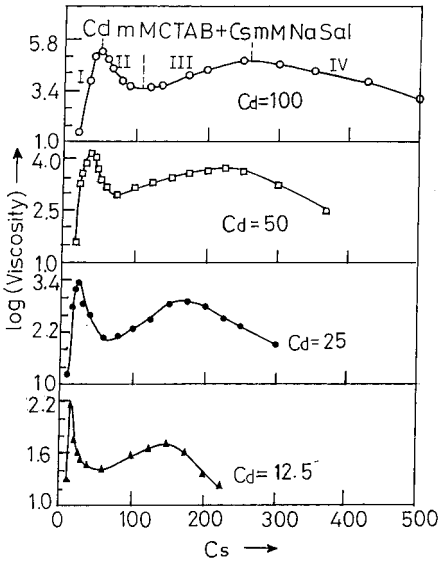

Figure 1. Zero-shear viscosity of CTAB/NaSal solutions as a function of NaSal concentration for surfactant concentrations of 12.5, 25, 50, and 100 mM.

Results and Discussion

I. Viscosity Measurements. The zero-shear viscosity of CTAB/NaSal solutions as a function of NaSal concentration at different surfactant concentrations is shown in Figure 1. The measurements are from surfactant concentrations of $C_d = 12.5$,

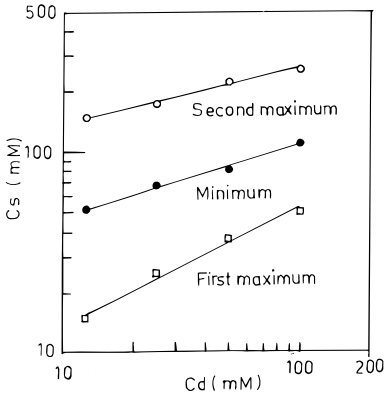

Figure 2. Log−log plot of NaSal concentrations at viscosity maxima and minimum as a function of surfactant concentration.

25, 50, and 100 mM. For each surfactant concentration, the viscosity curve shows a double-peak behavior. The viscosity curves can be divided into four different NaSal concentration (C_s) regimes for each value of C_d. In the region I, viscosity starts to rise steeply and reaches a maximum. The value of C_s/C_d, where η shows the first maximum, increases with the surfactant concentration. In region II, the viscosity decreases as the NaSal concentration is increased. In the beginning of region III, viscosity is a minimum. It is seen that the viscosity is still much higher than that of the water. At the minimum, the value of η, C_s/C_d is larger than 1 irrespective of the surfactant concentration. After passing the minimum, the viscosity starts to rise again and reaches a second maximum. When the NaSal concentration is further increased, the viscosity decreases again in region IV and attains low values at high concentrations.

The value of C_s at the first viscosity maximum varies with the surfactant concentration C_d. The maximum in viscosity seems to occur when micellar charge is fully neutralized by the Sal^- ions. The way NaSal concentration varies with surfactant concentration at the first viscosity maximum is shown in Figure 2. In the log−log plot we observe a single straight line between these two concentrations. Similiar observations have also been observed with CPyCl/NaSal solutions.[25] The relationship obtained is

$$\log(C_s) = 0.57 + 0.58 \log(C_d) \quad (9)$$

where C_s and C_d are expressed in mM units.

Similar results are found for the minimum and the second maximum of the viscosity. The concentration of NaSal for the minimum of the zero-shear viscosity with surfactant concentration varies as

$$\log(C_s) = 1.33 + 0.35 \log(C_d) \quad (10)$$

For the second maximum of the zero-shear viscosity, the relationship is

$$\log(C_s) = 1.87 + 0.27 \log(C_d) \quad (11)$$

II. SANS Measurements. The SANS technique has been extensively used to study micellar solutions.[26,27] This technique provides information about the shapes and sizes of the micelles and the parameters of the interaction between the micelles. The scattering profile for dilute solutions monotonically decreases and eq 2 is used to determine the shapes and sizes of the micelles. The expressions for the calculation of the form factor $F(Q)$ for different shapes and sizes of the particles are available.[23] In cases when the interparticle interactions are

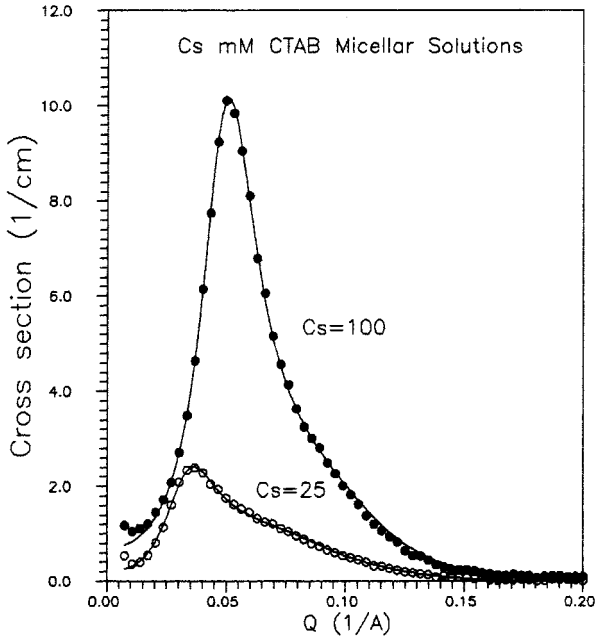

Figure 3. SANS distributions from pure 25 and 100 mM CTAB micellar solutions. Solid lines are theoretical fits based on Hayter and Penfold type analysis.

significant, eq 1 is used to obtain the micelle parameters. Various analytical methods are known to calculate interparticle structure factor $S(Q)$ for spherical particles.[28−31] The methods to compute $S(Q)$ for rigid rodlike micelles are, however, not yet developed. SANS data are usually analyzed to obtain the length and radius of rodlike micelles by assuming $S(Q) = 1$. This approximation is reasonably valid at low surfactant concentrations, in particular with salt.

The SANS distributions from pure 25 and 100 mM CTAB solutions are shown in Figure 3. These distributions show a correlation peak and indicate the presence of electrostatic interactions between the micelles. The theoretical fit to the experimental data in the figure is based on Hayter and Penfold type analysis, similar to that which has been reported in our earlier papers.[32,33] The aggregation numbers in these solutions are 130 for 25 mM CTAB and 155 for 100 mM CTAB and are in good agreement with those reported in the literature.[33,35] Micelles are slightly elongated. The value of the minor axis (22 Å) is independent of surfactant concentration, but the values of the axial ratio are 1.65 and 1.95 for CTAB concentrations of 25 and 100 mM, respectively. It seems that the solutions are reasonably monodispersed. The polydispersity, which has been determined using the Schultz distribution, is about 15%. The fractional charge per monomer (α) of the micelles is 0.19 and 0.22, respectively, in the two solutions. This perhaps is the reason for higher value of CS/C_d at the first viscosity maximum for 25 mM than that for 100 mM CTAB solution. The higher value of α for a pure CTAB solution means more NaSal will be required to neutralize the charge on the micelle.

The SANS measurements for 25 mM CTAB solution beyond the first viscosity maximum were carried out for the NaSal concentrations of 35, 50, 70, 125, 175, 225, and 300 mM, which have been selected from the different regimes of the viscosity curve. All SANS distributions are found to be similar. Figure 4 shows typical data, where SANS data for 25 mM in the presence of 70 mM NaSal are plotted on a log−log scale. We observe that there is straight part in the scattering data, and it exhibits a slope of ∼−1.0. This suggests that micelles are rigid rods, as the scattered intensity for a flexible linear object

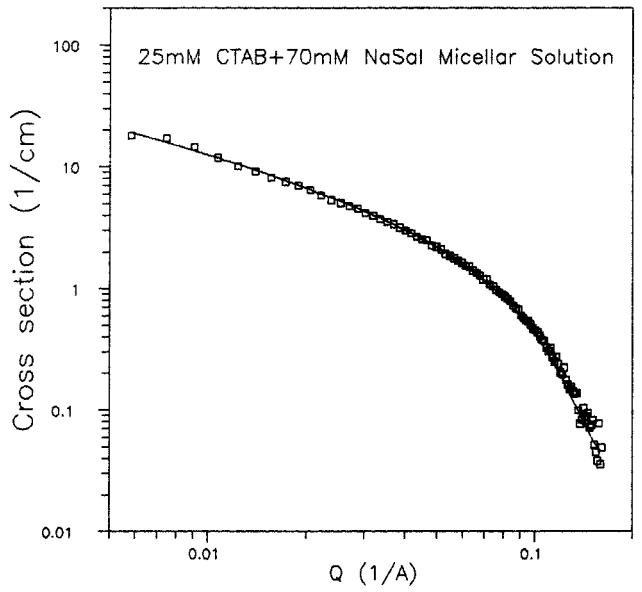

Figure 4. SANS distribution from 25 mM CTAB solution with 70 mM NaSal concentration. Solid line is theoretical fit using eq 5. All the SANS distributions corresponding to different C_s values beyond the first viscosity maximum for 25 mM CTAB solution are similar to this distribution.

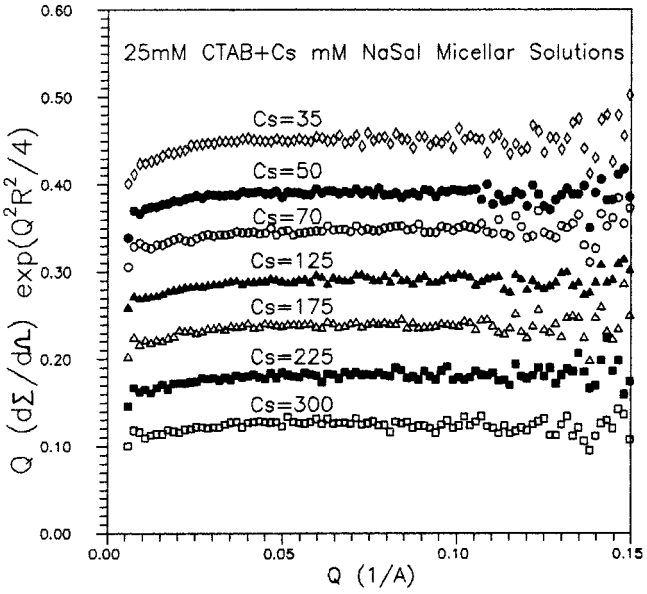

Figure 5. Scaled SANS data by the form factor of long rod for 25 mM CTAB at various NaSal concentrations beyond the first viscosity maximum. The data for C_s = 35, 50, 70, 125, 175, and 225 are shifted vertically by 0.30, 0.25, 0.20, 0.15, 0.10, and 0.05 units, respectively.

decreases faster than $1/Q$. For example, a polymer with excluded volume would have $I(Q) \sim 1/Q^{1.67}$ and a polymer with Gaussian coil structure $I(Q) \sim 1/Q^{2}$.[34] Thus, we believe that the structure of micelles in these solutions is actually quite different from that of polymer chains. This has been further confirmed by plotting $C(Q) = Q(d\Sigma/d\Omega)\exp(Q^2R^2/4)$ vs Q graphs (Figure 5). A $C(Q)$ vs Q graph should be constant, which is determined by the radius of the rodlike micelle. In Figure 5 we note that $C(Q)$ is constant for 25 mM solution for all NaSal concentrations for which the measurements have been made. The radius of the micelle is obtained to be 22 ± 1 Å.

Figure 6 shows $C(Q)$ vs Q graphs for 100 mM CTAB solutions with varying concentrations of NaSal. It is seen that these results are different from those for 25 mM CTAB solutions

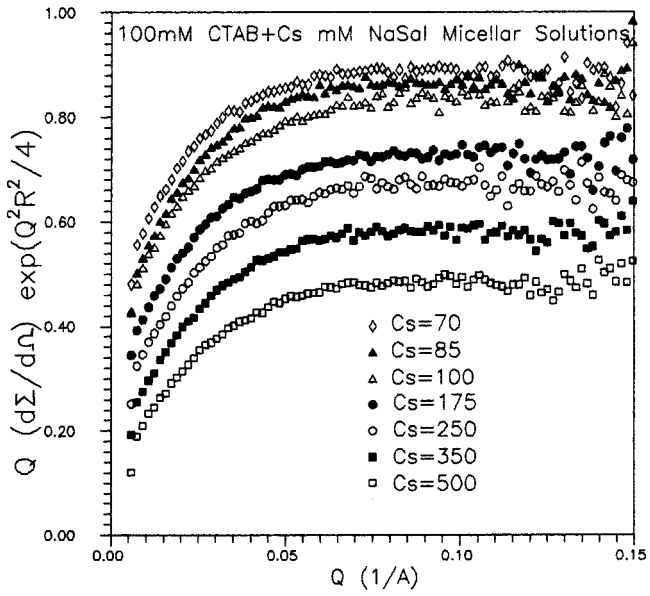

Figure 6. Scaled SANS data by the form factor of long rod for 100 mM CTAB at various NaSal concentrations beyond the first viscosity maximum. The data for C_s = 70, 85, 100, 175, 250, and 350 are shifted vertically by 0.30, 0.25, 0.20, 0.15, 0.10, and 0.05 units, respectively.

(Figure 5). $C(Q)$ gradually falls as one goes to low Q-values. This is due to the presence of the electrostatic interaction between the micelles and suggests that intermicellar interference cannot be neglected in these solutions. However, it will be a good approximation to assume that there is negligible interference between the micelles in the case of 25 mM CTAB/NaSal solutions.

The fact that micelles are rodlike and that the intermicellar interference is not important in 25 mM CTAB solutions, SANS data from 25 mM CTAB/NaSal solutions have been analyzed by combining eqs 3 and 5. Unlike in the case of pure CTAB solutions, where micelles are nearly monodispersed, we find that micelles are highly polydispersed in the presence of NaSal. The polydispersity as obtained by the Schultz distribution is 100%. At such high polydispersity, the Schultz distribution (eq 6) reduces to the exponential distribution (eq 8). That is, the length distribution of micelles in CTAB/NaSal solutions follows an exponential distribution. The theoretical models predict that, for living polymers, their length distribution is exponential. This suggests that micellar structure in CTAB/NaSal solutions beyond the first viscosity maximum is consistent with the living polymers model. The mean length of living polymers in all these solutions have been obtained to be 500 ± 50 Å.

We have seen that intermicellar interference is not negligible for 100 mM CTAB/NaSal solutions. It is seen that intensity drops in the low Q-region for these solutions as the NaSal concentration is increased (Figure 7). We believe that micellar structure is not changing with NaSal concentration beyond the first viscosity maximum as has been observed with 25 mM CTAB/NaSal; the changes in SANS distributions are expected to be due to change in the intermicellar interactions. The data, however, could not been analyzed as no proper method is available to incorporate the intermicellar structure factor for the rodlike charged micelles. We see that micellar structure in CTAB/NaSal solutions as obtained by SANS are almost same beyond the first viscosity maximum in η vs C_s curves. However, the zero-shear viscosity varies with increase in NaSal concentration. Similar results, nonvariation of micellar structure for the high values of C_s/C_d, have also been reported by the cryo-TEM measurements.[14] This is not surprising, as the

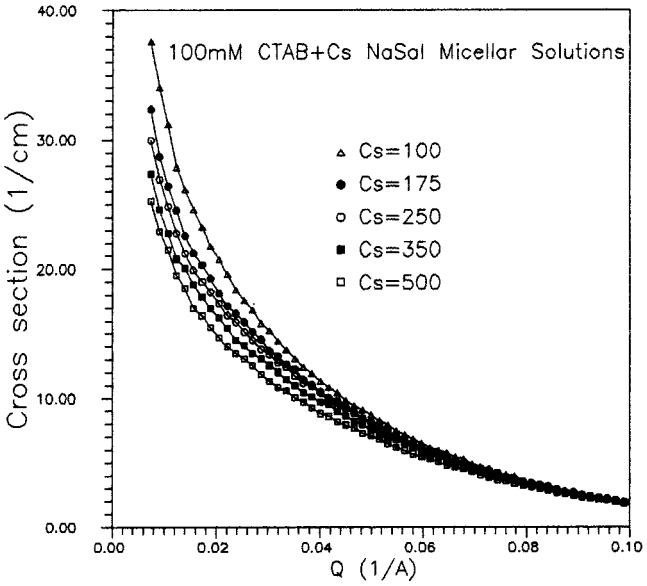

Figure 7. SANS distributions for 100 mM CTAB solution at different NaSal concentrations beyond the viscosity minimum. The solid lines are the hand-drawn curves to indicate the differences between various SANS distributions.

parameters that govern the viscosity are not only micellar sizes but also intermicellar interactions and the kinetic processes taking place in the solutions.[1,2]

Conclusions

The viscoelastic CTAB/NaSal micellar solutions have been studied by SANS and viscosity measurements as a function of NaSal concentration at various surfactant concentrations. The zero-shear viscosity of these solutions as a function of NaSal concentration shows a double-peak behavior. The NaSal concentrations at two maxima and a minimum between them in the viscosity curves vary linearly with surfactant concentration on a logarithmic scale. SANS measurements from the solutions beyond the first viscosity maximum show that micelles are rigid rods and highly polydispersed. The length distribution of the micelles is exponential, indicating that micelles behave as living polymers beyond the first viscosity maximum. Further, SANS measurements suggest that micellar structures are independent of C_s beyond the first viscosity maximum. The changes seen in η vs C_s curves beyond first viscosity maximum are perhaps connected with the changes in the intermicellar interactions.

References and Notes

(1) Cates, M. E.; Candau, S. J. *J. Phys.: Condens. Matter* **1990**, *2*, 6869.
(2) Rehage, H.; Hoffmann, H. *Mol. Phys.* **1991**, *74*, 933.
(3) Shikata, T.; Hirata, H.; Kotaka, T. *Langmuir* **1987**, *3*, 1081.
(4) Candau, S. J.; Hirsch, E.; Zana, R.; Delsanti, M. *Langmuir* **1989**, *5*, 1225.
(5) Imae, T. *Colloid Polym. Sci.* **1989**, *267*, 707.
(6) Sasaki, M.; Imae, T.; Ikeda, S. *Langmuir* **1989**, *5*, 211.
(7) Gamboa, C.; Sepulveda, L. *J. Colloid Interface Sci*. **1986**, *113*, 566.
(8) Olsson, U.; Soderman, O.; Guering, P. *J. Phys. Chem.* **1986**, *90*, 5223.
(9) Menon, S. V. G.; Goyal, P. S.; Dasannacharya, B. A.; Paranjpe, S. K.; Mehta, R. V.; Upadhyay, R. V. *Physica B* **1995**, *213*, 604.
(10) Goyal, P. S.; Dasannacharya, B. A.; Kelkar, V. K.; Manohar, C.; Rao, K. S.; Valaulikar, B. S. *Physica B* **1991**, *174*, 196.
(11) Shikata, T.; Sakaiguchi, Y.; Uragami, H.; Tamura, A.; Hirata, H. J. *Colloid Interface Sci*. **1987**, *119*, 291.
(12) Imae, T. *J. Phys. Chem.* **1990**, *94*, 5953.
(13) Wu, X.-I.; Yeung, C.; Kim, M. W.; Huang, J. S.; Ou-Yang, D. *Phys. Rev. Lett*. **1992**, *68*, 1426.
(14) Clausen, T. M.; Vinson, P. K.; Minter, J. R.; Davis, H. T.; Talmon, Y.; Miller, W. G. *J. Phys. Chem.* **1992**, *96*, 474.
(15) Lin, Z.; Cai, J. J.; Scriven, L. E.; Davis, H. T. *J. Phys. Chem.* **1994**, *98*, 5984.
(16) Lin, Z.; Scriven, L. E.; Davis, H. T. *Langmuir* **1992**, *8*, 2200.
(17) Cummins, P. G.; Staples, E.; Hayter, J. B.; Penfold, J. *J. Chem. Soc., Faraday Trans. 1* **1987**, *83*, 2773.
(18) Penfold, J.; Staples, E.; Cummins, P. G. *Adv. Colloid Interface Sci*. **1991**, *34*, 451.
(19) Marignan, J.; Appell, J.; Bassereau, P.; Porte, G.; May, R. P. *J. Phys. (Paris)* **1989**, *50*, 3553.
(20) Lin, M. Y.; Hanley, H. J. M.; Sinha, S. K.; Straty, G. C.; Peiffer, D. G.; Kim, M. W. *Physica B* **1995**, *213*, 613.
(21) Epperson, J. E.; Carpenter, J. M.; Crawford, R. K.; Thiyagarajan, P.; Klippert, T. E.; Wozniaik, D. G. Unpublished work.
(22) Hayter, J. B.; Penfold, J. *Colloid Polym. Sci.* **1983**, *261*, 1022.
(23) Guinier, A.; Fournet, G. *Small Angle Scattering of X-rays*; Wiley Interscience: New York, 1955.
(24) Kotlarchyk, M.; Chen, S. H. *J. Chem. Phys*. **1983**, *79*, 2461.
(25) Rehage, H.; Hoffmann, H. *J. Phys. Chem.* **1988**, *92*, 4712.
(26) Chen, S. H. *Annu. Rev. Phys. Chem*. **1986**, *37*, 351.
(27) Goyal, P. S. *Phase Transitions* **1994**, *50*, 143.
(28) Hayter, J. B.; Penfold, J. *Mol. Phys*. **1981**, *42*, 109.
(29) Benmouna, M.; Weill, G.; Benoit, H.; Akcasu, Z. *J. Phys*. **1982**, *43*, 1679.
(30) Baba-Ahmed, L.; Benmouna, M.; Grimson, M. *J. Phys. Chem. Liq*. **1987**, *16*, 235.
(31) Chen, S. H.; Sheu, E. Y.; Kalus, J.; Hoffmann, H. *J. Appl. Crystallogr*. **1988**, *21*, 751.
(32) Aswal, V. K.; Goyal, P. S.; Menon, S. V. G.; Dasannacharya, B. A. *Physica B* **1995**, *213*, 607.
(33) Goyal, P. S.; Menon, S. V. G.; Dasannacharya, B. A.; Rajagopalan, V. *Chem. Phys. Lett*. **1993**, *211*, 559.
(34) Higgins, J. S.; Benoit, H. C. *Polymers and Neutron Scattering*; Clarendon Press: Oxford, 1994.
(35) Berr, S. S. *J. Phys. Chem.* **1987**, *91*, 4760.